IOP Publishing Measurement Science and Technology
Meas. Sci. Technol. **32** (2021) 114001 (12pp) https://doi.org/10.1088/1361-6501/ac0f23

Application of 3-omega method for thin-film heat flux gauge calibration

Shawn Siroka*, Brian M Foley, Reid A Berdanier and Karen A Thole

Department of Mechanical Engineering, Penn State University, State College, PA 16801, United States of America

E-mail: sis5702@psu.edu

Received 1 April 2021, revised 7 June 2021
Accepted for publication 28 June 2021
Published 13 July 2021

Abstract

Double-sided thin-film resistance temperature detector (RTD) heat flux gauges (HFGs) are commonly used to characterize heat transfer rates in high-heat flux environments with complex flow features. These gauges comprise two thin-film RTDs on opposing sides of a dielectric. To deduce accurate heat flux, the RTDs must be properly calibrated and the material properties of the dielectric must be characterized. This study presents a complete gauge characterization method for sensors of this type by applying standard calibration procedures with specially-designed RTDs capable of utilizing the 3-omega method. The 3-omega method quantifies the thermal conductivity and thermal product of a material by measuring the response of a specially designed heater/thermometer deposited on the substrate. This study shows the 3-omega method enables RTD calibrations and thermal property determination over a range of temperatures for individual gauges, reducing the uncertainty in calculated heat flux. Although the method is quite general, this study utilized platinum RTDs with a polyimide dielectric, which is common in turbomachinery applications. The thermal properties obtained through this method agree with previous characterization efforts; however, discrete characterization of seven gauges shows that gauge-to-gauge variation in the dielectric could influence measured heat flux by as much as 30%. This study also builds the framework to characterize the thermal conductivity of the adhesive layer beneath the gauge which is necessary to mount the sensors to the test article. Although often uncharacterized, the adhesive thermal conductivity has a significant impact on matching experimental measurements to simulations. Additionally, this study found that if the thermal conductivity of the dielectric is constant (an assumption that holds for the present study), an *in-situ* RTD calibration can be performed. *In-situ* RTD calibration and traditional method RTD calibration agreed to within 0.1%. Overall, this work has practical implications in obtaining high quality measurements from HFGs of this type.

Keywords: heat flux gauges, turbomachinery instrumentation, thermal property characterization

(Some figures may appear in colour only in the online journal)

Nomenclature

b	Heater half width
c	Volumetric specific heat
d	Thickness
f	Frequency $= 0.5\,\pi^{-1}\omega$
I	Current
j	Imaginary number $= \sqrt{-1}$
k	Thermal conductivity
L	Heater length
R	Resistance
V	Voltage
X	In-phase transfer function
Y	Out-of-phase transfer function

Greek

α_R	Coefficient of resistance
α_T	Thermal diffusivity $= kc^{-1}\rho^{-1}$

* Author to whom any correspondence should be addressed.

 © 2021 IOP Publishing Ltd Printed in the UK

γ	Wave number $= j\lambda^{-1}$
δ	Perturbation in quantity
Δ	Change in quantity
ξ	fitting constant ≈ 0.922
ε	Percent error
ρ	Density
η	Integration variable
λ	Thermal wave length $\sqrt{D\pi^{-1}f^{-1}}$
ω	Angular frequency $= 2\pi f$

Subscripts and Accents

0	Amplitude
1	Related to the first harmonic
2	Related to the second harmonic
3	Related to the third harmonic
a	Related to the adhesive
an	Annealed state
bot	Bottom gauge quantity
e	Zero-current value
in	Initial state
n	Related to an arbitrary harmonic
ref	Reference state
rms	Root mean square value
s	Related to substrate/dielectric
set	Set point
sys	System quantity
top	Top gauge quantity
ω	Related to angular frequency

1. Introduction

Heat flux measurements aid in understanding the time-resolved thermal performance of a system and are critical to improving thermal designs in a wide range of applications. Although several types of heat flux measurement devices exist, this paper focuses on the calibration of double-sided thin-film resistive temperature detector (RTD) heat flux gauges (HFGs) shown in figure 1, sensors of this type are composed of two RTDs on opposing sides of a dielectric and have been established for high heat flux environments in complex flow fields [1, 2].

Double-sided thin-film RTD HFGs use thermo-electrical calibrations and material properties to deduce a heat flux. The RTDs are supplied by a small excitation current, and the corresponding resistance is related to a temperature through an electrothermal calibration traditionally completed in a stable temperature environment such as a scientific convection oven or oil bath. This calibration allows transformation of the measured quantity (voltage or resistance) of the platinum RTD to temperature. The temperature traces from the top and bottom can then be used to deduce heat flux by solving the unsteady conduction equation with the material properties of the dielectric.

The ambiguity of these sensors is influenced by the RTD calibration accuracy as well as the accuracy of the thermal properties of the substrate. More specifically, highlighted in figure 1, the coefficient of resistance of the RTDs ($\alpha_{\mathrm{R,top}}$ and

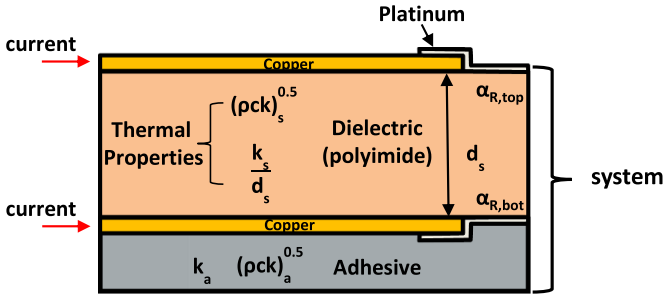

Figure 1. Schematic of double-sided heat flux gauge.

$\alpha_{\mathrm{R,bot}}$) as well as the thermal product $(\rho ck)_s^{0.5}$ and thermal conductivity over thickness (k_s/d_s) of the substrate must be known to properly deduce time-resolved heat flux [3]. Although previous researchers have successfully implemented appropriate characterization techniques for these parameters [1, 4–6], no technique currently characterizes the thermal properties for each individual HFG. Instead, bulk material properties are tested and assumed to represent the sensor dielectric. However, batch-to-batch variations and mismatches in characterization and gauge operation temperature can lead to inaccuracies in the thermal properties of up to 20% which propagates to errors in heat flux measurements [7]. Additionally, no existing method allows for an *in-situ* calibration of the RTDs which could drift as the metal anneals or degrades in high temperature environments.

The 3-omega method [8, 9] provides a new approach to improve upon traditional HFG calibration techniques. The 3-omega method quantifies the thermal conductivity and thermal product of a material by measuring the response of a specially-designed heater/thermometer deposited on the substrate. Because thin film RTD HFGs require deposition of metal strips, this technique lends itself well for characterizing the thermal properties of the dielectric. Furthermore, since the 3-omega method links the electrothermal response of the RTDs to the substrate thermal properties, an *in-situ* calibration of the RTDs is possible. Moreover, since RTDs on both sides of the dielectric are used, it is possible to obtain the thermal conductivity of the adhesive layer (k_a) as well which plays a key role in matching simulations to experimental results. Having the capability to check and alter calibrations *in-situ* on a per gauge basis will increase the accuracy of the measurement and save significant time and effort in implementing measurements of this type.

This paper presents a methodology for how the 3-omega technique can be used as an alternative to traditional thermal characterization of the dielectric and to supplement traditional RTD calibrations. First, the background information on the technique is presented. Next, the design and fabrication of sensors is introduced, and data reduction methods are illustrated. This procedure is then applied to seven double-sided thin-film RTD HFGs and thermal property results are obtained across a range of temperatures and compared to traditional method values. Finally, the technique is expanded to demonstrate *in-situ* calibrations.

2. Literature review

Thin film RTD HFGs have been used for decades in the turbomachinery discipline to characterize the heat transfer in complex flow fields. Typically, these sensors have used polyimide as the dielectric material and a platinum deposition on the order of nanometers for the metal deposition [1, 2, 5, 6, 10]. These selections allow the sensors to be flexible enough to wrap around complex airfoil geometries with a time response on the order of kilohertz which is critical to characterize harmonics of blade passing events present in turbomachinery flows [10–15]. Noteworthy research by a host of institutions over the last several decades has advanced the design and fabrication of these type of sensors [1, 5–7, 11]. For this reason, the current study focuses on platinum RTD elements on both sides of a polyimide dielectric and their application to turbomachinery. However, the general process holds for other materials as well. This paper demonstrates the use of the 3-omega technique for the new purpose of creating a more accurate thin-film RTD HFG. For that reason, the literature review will draw from both 3-omega literature, nanoscale platinum film studies, and previous HFG applications.

A stable calibration is necessary for an RTD to obtain accurate measurements. This calibration depends on the temperature coefficient of resistance, α_R (constant for platinum), as well as the reference resistance of the RTD (R_{ref}). The bulk platinum α_R value is 3.9×10^{-3} (°C^{-1}) [16] and directly characterizes the sensitivity of RTDs. However, residual stresses and electron scattering at grain and film boundaries resulting from the deposition process for thin film RTDs cause the coefficient of resistance of thin film sensors to deviate from bulk values.

Tiggelaar *et al* [17] tested the stability of thin platinum RTDs deposited onto silicon wafers showing an annealing process with a ramp of 10 °C min^{-1} up to 950 °C relaxes the residual stresses while increasing the grainsize of the platinum film. Similarly, Chung and Kim [18] showed annealing a thin platinum film at 1000 °C for 2 h resulted in stable physical and electrical structures as well as α_R values near the expected bulk platinum property. Zribi *et al* [19] further analyzed the annealing of thin film RTD HFGs using glass as the dielectric. Zribi *et al* obtained stable thin platinum α_R values through an annealing process of 250 °C, but with values of α_R roughly one-third that of bulk values.

In many cases, including the present study, the annealing process is limited by the maximum allowable temperature for the dielectric. As a consequence, manufacturers of flexible RTD HFGs are constrained to α_R values lower than bulk platinum [7] due to the use of polyimide as the dielectric. However, accurate measurements have been demonstrated from stable and repeatable coefficient of resistance values that deviate from bulk values [7] so long as the α_R value is properly characterized.

Apart from RTD calibrations, the thermal properties of the dielectric, including (k_s/d_s) and $(\rho ck)_s^{0.5}$, must be known to achieve accurate heat flux measurements. Experimentally, these lumped parameters can be quantified by measuring the thermal response of the thin film RTD HFG to a known heat source. Many types of heat sources have been previously used, but a convective heat source has been found to be the most reliable and closest to experimental conditions [4, 5]. Lumped parameter thermal property determination allows reliable data at a particular temperature, but is rarely expanded for a range of temperatures. Alternatively, these parameters can also be independently tested [6, 7] through a number of standards [20, 21]. Both the lumped parameter and independent methods are valid ways of quantifying these thermal properties, but neglect variations by individual thin-film RTD HFGs.

One experimental method that could be used in place of the traditional standards is the 3-omega method for thermal conductivity. Developed by Cahill *et al* [8], this method quantifies the thermal conductivity of a material by measuring the harmonic response to a heater. Through this technique, it is also possible to determine the thermal diffusivity and therefore the thermal product of the material [22]. The 3-omega method relies upon characterizing the relationship between the coefficient of resistance of the heater and the thermal properties of the dielectric, thereby making it particularly useful for thin film RTD HFG calibration.

Below the sensor, an adhesive layer is necessary to bond the thin film RTD HFG to the test article. In addition to the dielectric thermal properties, the thermal properties of the adhesive layer are vital to scaling results to engine conditions as well as matching experiment to models. Ni *et al* [23], compared experimental data from thin film RTD HFGs to an engine simulation. When accounting for the presence of an insulating adhesive layer, experimental results better matched numerical models. Through the use of both sides of a double-sided thin-film RTD HFG, it is possible to characterize the material properties of the underlying adhesive.

Although the application of the 3-omega process is novel to thin film RTD HFGs, bidirectional 3-omega sensors have been successfully used in the past to quantify underlying materials. Lubner *et al* [24] utilized the principles of the 3-omega method to create bi-direction sensors. In this configuration, sensors first quantify the backing material; then, a sample with an unknown thermal conductivity is placed on the exposed sensor. Through prior quantification of the backing material, the unknown material properties can then be deduced. A comparison can be drawn between the Lubner *et al* approach and the application of double-sided thin-film RTD HFGs: first, the top sensor quantifies the thermal properties of the dielectric; then, the bottom sensor is used in conjunction with the thermal properties of the top sensor to quantify the underlying material.

The current study adds to the available literature by combining techniques from various disciplines to create a unique calibration method for double-sided thin-film RTD HFGs. This technique can be utilized across a variety of disciplines to better quantify heat flux, leading to more robust and efficient thermal systems.

3. Theoretical framework for 3-omega method

The theoretical framework for the 3-omega technique specific to HFGs is summarized in this section, and the reader is

directed to previous works for further details and derivation of the governing relations [8, 9, 22]. In general, the electrical and thermal transfer functions of a system can be related by using a combined heater/thermometer to excite the system and measure the response. Following the procedure outlined by Dames and Chen [9], the measured quantities of harmonic voltage drop across the heater ($V_{n\omega,\mathrm{rms}}$), the coefficient of resistance of the heater (α_R), the zero-current resistance of the heater (R_e), and the current driving the heater $I_{1,\mathrm{rms}}$ can be related to the electric transfer function through equation (1):

$$\frac{V_{n\omega,\mathrm{rms}}}{\alpha_\mathrm{R} R_\mathrm{e}^2 I_{1,\mathrm{rms}}^3} = X_n(\omega_1) + j\, Y_n(\omega_1) \tag{1}$$

where $X_n(\omega_1)$ is the in-phase component of the transfer function and $Y_n(\omega_1)$ is the out-of-phase component. Both components can be a function of the current-driving frequency, ω_1 and are denoted for a specific harmonic, n. The components of the electrical transfer function contain valuable information about the thermal properties of the system.

As presented here, equation (1) can be applied to a variety of geometries and harmonics. The geometry relevant to this study is a line heater above a substrate and will focus on the in-phase third harmonic system response. This formulation is considered the traditional case for the 3-omega method [8] and has been shown to produce robust measurements of thermal conductivity [9].

To apply the 3-omega technique, a properly-designed heater/thermometer must be supplied with a sinusoidal current at frequency ω_1 which introduces Joule heating and a corresponding temperature rise at a harmonic frequency, ω_2. In turn, this process creates a voltage across the heater/thermometer that has a dominating ω_1 component with a small ω_3 component. It has been shown by solving the conduction equation [22] that the third-harmonic electric transfer functions, X_3 and Y_3 can be related to the thermal properties through equation (2) such that

$$X_3(\omega_1) + Y_3(\omega_1) = \frac{1}{4\pi L k} \int_0^\infty \frac{\sin^2(\eta b)}{(\eta b)^2 \sqrt{\eta^2 + \gamma(\omega)^2}} \mathrm{d}\eta \tag{2}$$

where k is the thermal conductivity, η is an integration variable, γ is the wave number, b is the heater half-width, and L is the heater length. Equation (2) has no known closed-form solutions and must be approximated numerically. Therefore, X_3 is commonly simplified in the limiting case that the heater half-width is much smaller than the thermal penetration depth (λ_s) defined by

$$\lambda_\mathrm{s} = \sqrt{\frac{2\alpha_\mathrm{T}}{\omega_1}} \tag{3}$$

where α_T is the thermal diffusivity and ω_1 is the heating frequency in radians per second.

The thermal penetration depth defined in equation (3) is an important parameter since it quantifies the penetrating distance into a substance for an oscillating thermal wave. If $b \ll \lambda_\mathrm{s}$, equation (2) can be simplified such that X_3 is directly related to the thermal properties through equation (4)

$$X_3(\omega_1) \cong \frac{1}{8\pi L k}\left(\ln(\omega_1) + \ln(2) + \ln\left(\frac{b^2}{\alpha_T}\right) - 2\xi\right) \tag{4}$$

where α_T is the thermal diffusivity and ξ is a fitting constant. From equation (4), it is possible to use the measured $X_3(\omega_1)$ and the geometry of the heater to solve for the thermal parameters of interest, k and D. The linear relation of X_3 and $\ln(\omega)$ correlates the slope to the thermal conductivity and subsequently the intercept to thermal diffusivity. Once thermal conductivity and diffusivity are known, it is possible to obtain the thermal product, $\sqrt{\rho c k}$ through equation (5)

$$\sqrt{\rho c k} = \sqrt{\frac{k^2}{\alpha_\mathrm{T}}}. \tag{5}$$

4. HFG design for 3-omega method

Thin film RTD HFGs already utilize nanofabrication processes to create the thin-film RTDs on the dielectric surface. However, optimization of the RTD geometry is required for the 3-omega method to be implemented. Equation (4) denotes a simplified relationship which only applies under certain assumptions: an infinitely long heater, an isothermal substrate, the heater as a line source; and the substrate is semi-infinite.

To fulfill these assumptions, the heater/thermometer length and width must be chosen to ensure a sufficient linear region exists. In practice, the robustness of the gauges and the presence of this linear region are negatively correlated. Therefore, the heater/thermometer design of these gauges need to maximize gauge durability without compromising the measurements. Dames *et al* outlines several design guidelines to ensure a linear region exists for a range of measurement accuracy [25]. Table 1 outlines these common design criteria recommended to apply the 3-omega method with the simplified equation (2).

In table 1, the geometric properties of the gauge (d_s, L, and b) must be chosen to ensure that λ_s can be modulated through a sinusoidal current frequency sweep to meet the above assumptions. Based on information in table 1, an excitation frequency range exists for which the gauges in this study meet most recommendations except for the semi-infinite approximation. Combining assumption 1 with assumption 2, it can be shown that $d_\mathrm{s}/b > 3.2$ to meet all assumptions. For a specified polyimide substrate material, the thickness d_s is fixed, which leaves b as the varying parameter. However, decreasing values of b correlate directly with increased manufacturing challenges and reduced durability of the gauge. For this study, the value for b was chosen in accordance with previous survivability tests. Since the guild line to meet assumption 1 in table 1 was not achieved for the current design, further validation of the linear post processing is warranted and will be addressed in subsequent sections.

Table 1. Criteria for 5% error in linear approximation [25].

Assumption	Guild line	HFG design
1. Substrate is semi-infinite ($d_S \to \infty$) [26]	$d_s/\lambda_s \geqslant 2$	1.02
2. Substrate sees heater as line source ($b \to 0$) [27]	$\lambda_s/b \geqslant 1.6$	1.6
3. Heater is infinitely long ($L \to \infty$) [26]	$L/\lambda_s \geqslant 10$	10

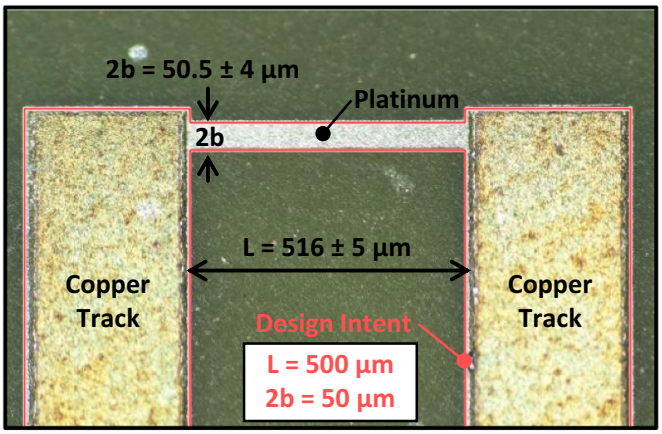

Figure 2. Design and fabrication of top-side of HFG with ranges for minimum and maximum measurements in tested geometries.

Following the design parameters listed in table 1, figure 2 illustrates the HFG geometry selected for this study with the measured mean fabrication values as well as the range. As illustrated in figure 1 (side view) and figure 2 (top view), a 50 µm polyimide copper-clad film was etched to create the copper leads, and platinum was subsequently deposited via a vapor deposition process to a targeted thickness of 1500 Å. This deposition resulted in RTD resistance values of 40–135 Ω. The variation in resistance most likely stems from deviations in thickness and microstructure in the deposited film. However, these variations are accounted for in the 3-omega process and therefore did not affect the conclusions of this study. Further details about the gauge fabrication are discussed by Siroka *et al* [7].

Figure 2 shows the design intent as an outline with the measured values obtained after fabrication via a microscope. The dimensional stability of b and L is limited by the mask fabrication for the specific contact lithography technique used in this study. A range of 10 µm was measured in the length while a range of 8 µm was measured in the width. Since the geometry of the heater is used to deduce the thermal properties, each individual gauge in this study was measured to ensure high accuracy in the results.

5. HFG calibration procedure

Thin-film RTD HFGs require electrothermal RTD calibrations to accurately transform from measured voltage or resistance to temperature. These gauges also require thermal properties

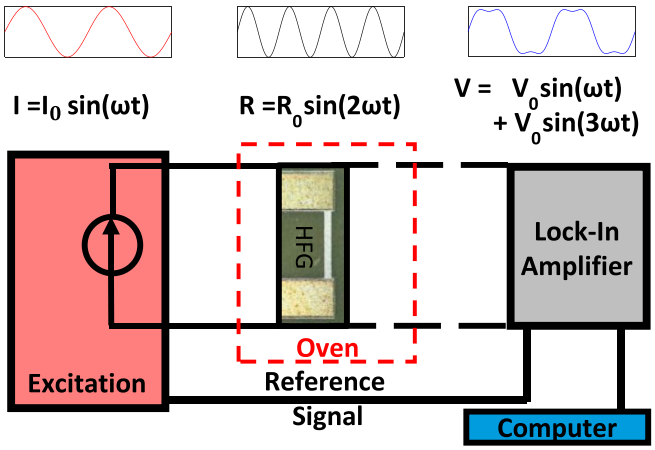

Figure 3. Calibration setup capable of sweeping temperature to simultaneously determine the electrothermal calibration and the thermal properties.

to translate measured temperature values on the top and bottom side of the gauge into heat flux. This section provides a framework for implementing the 3-omega technique to characterize double-sided thin-film RTD HFG thermal properties during a traditional calibration process. Specifically, this section focuses on how the top-side thin-film RTD calibration can be used in conjunction with the 3-omega method to determine thermal properties of the dielectric. However, during this process, the bottom-side HFG is also calibrated and information about the underlying adhesive layer can be gathered which will be covered in a following section.

For the electrothermal RTD calibrations, the gauges were excited by a 1 mA constant current while situated in a scientific convection oven with a stability rating of 0.2 K. Once the oven and gauges reached thermal equilibrium, RTD voltages were collected to represent baseline calibration data. The excitation was then switched to a sinusoidal current to utilize the 3-omega method and determine the thermal properties. Then, the temperature was changed to the next setpoint and the process was repeated. For this experiment, the temperature ranged from 50 °C to 150 °C.

Figure 3 illustrates the experimental setup for the calibration procedure. On the right of figure 3, specialized excitation and filtering equipment capable of switching between a constant current operation mode and a sinusoidal excitation is labeled as excitation. For the 3-omega technique, a lock-in amplifier was required to separate the small-amplitude third harmonic voltage from the fundamental first harmonic. The lock-in amplifier was connected to a computer through which the RMS values of both harmonics were recorded in reference to the gauge excitation. The system outlined here and shown in figure 3 allows for individual gauge calibrations to be conducted in a scientific oven. However, the same setup can be utilized *in-situ* to obtain thermal property measurements. The only difference between the calibration set-up and experimental use is the relocation of the instrumented test article from the oven to an experimental environment.

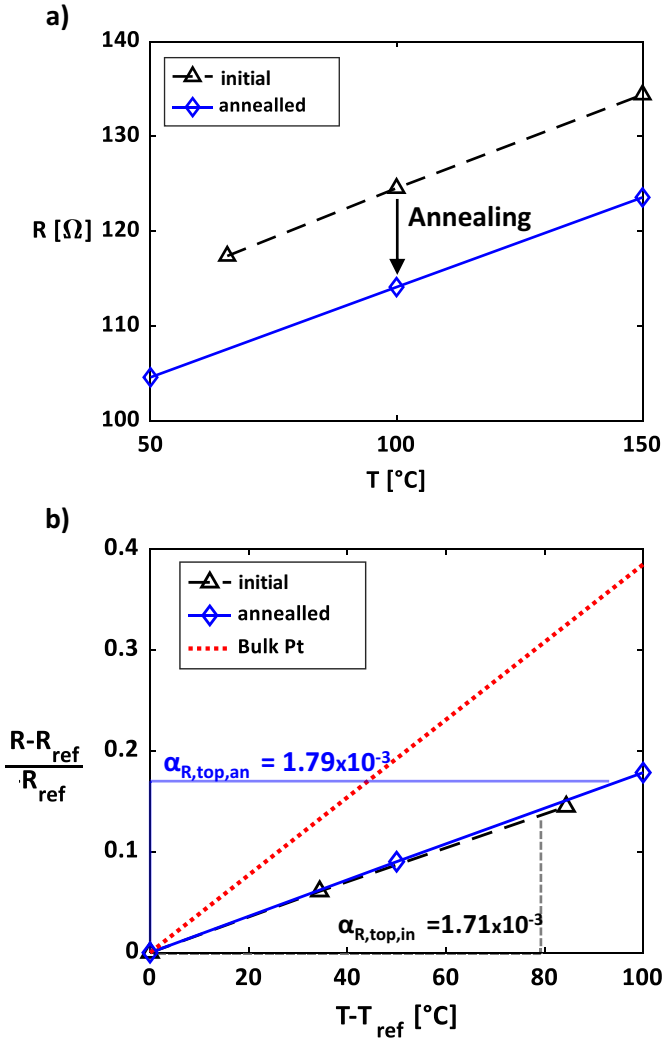

Figure 4. (a) Resistance versus temperature for a HFG before and after the annealing process. (b) Nondimentionalized results from figure (a) showing the effect of annealing on α_R.

5.1. Electrothermal calibration

The goal of the electrothermal calibration is to create a calibration curve for the RTD elements on the HFGs. Figure 4(a) shows two example calibration curves for the same gauge at different annealing states. The typical annealing procedure sets the oven slightly higher than the maximum calibration temperature until the nominal resistance of the gauge changes by less than 0.05% over the span of an hour. This annealing relaxes the internal stresses in the platinum RTD changing the platinum grain-size and therefore the resistance [17].

The curves in figure 4(a) give an understanding of the annealing process. From figure 4(a), the resistance of the RTD decreases as the internal stresses in the platinum relax at elevated temperature. Figure 4(b) shows the normalized resistance for the two curves in figure 4(a) as well as a curve relating to the bulk platinum coefficient of resistance. Notice that as the RTD is annealed, the coefficient of resistance increases, but still remains far from bulk values. As stated previously, this discrepancy arises because the polyimide backing constrains the maximum annealing temperature below what is required to reach bulk platinum value. Note that all the data in figure 4 as well as subsequent figures correspond to the same thin-film RTD HFG labeled subsequently as the reference gauge.

As shown in figure 4, the defined annealing process changes the resistance and α_R value for the RTD that results in errors in the absolute temperature measurement. The data in figure 4 confirm that RTDs require annealing. Furthermore, as these gauges are implemented for long-duration experiments, it is critical to have an *in-situ* calibration process to account for any calibration drift that arises due to RTD annealing or deterioration in the testing environment. As will be illustrated in subsequent section, the 3-omega technique provides a tool for such *in-situ* calibrations.

5.2. Three-omega thermal property determination

For each temperature setpoint in figure 4(a), the 3-omega technique was employed to quantify the thermal properties of the substrate for the annealed condition. A reference signal synced with the lock-in amplifier's internal oscillator was used to modulate the current excitation over a range of frequencies with a logarithmic spacing from 10 to 10 000 Hz. The first and third harmonic RMS voltage drop across the heater/thermometer was recorded by the lock-in amplifier with a filter setting and settling time automatically adjusted for each frequency. Each 3-omega sweep was completed in less than 3 min without requiring wiring changes.

An example frequency sweep is shown in figure 5 where the real and imaginary components from equation (1) are on the ordinate and the logarithm of the fundamental frequency is on the abscissa. The trace in figure 5 is for a gauge with a resistance of 125 Ω excited with a 10 mA amplitude sinusoidal current at 150 °C. This 3-omega sinusoidal excitation drives a current with an amplitude that is an order of magnitude larger than the constant current used for typical operating and electrothermal calibration. This relatively large current is necessary to create a detectable third harmonic voltage defined by the noise floor of the chosen electronic systems.

In figure 5, the measured in-phase and out-of-phase electric transfer function are plotted as asterisks and x's, respectively. While operating at relatively low frequencies, a region exists for where the in-phase component is linear and the out-of-phase component is constant. This linear region is illustrated in figure 5 by red circles and is defined as the region in which the assumptions listed in table 1 are best met through the HFG design column. The existence of the linear region builds validation that equation (3) can be used to quantify the thermal properties of the substrate. The red circles were used to calculate the thermal conductivity. It can be seen in figure 5 that including adjacent points into the linear region would have little effect on the calculated slope. This builds validation that the assumptions in table 1 are correct.

Figure 5 also illustrates the computational approximation to a more accurate version of equation (2) which accounts for multi-layered substrates [28], effectively accounting for layers below the gauge which may affect the system response if

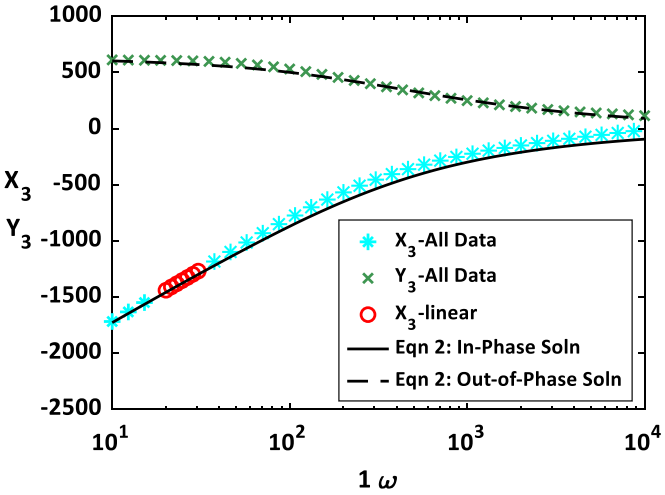

Figure 5. Measured gauge response for a 3-omega sweep comparing multilayer solution to linear trend.

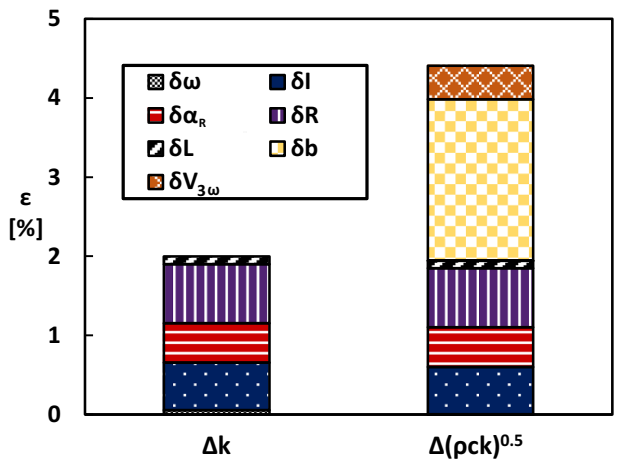

Figure 6. Bias uncertainty for thermal conductivity and thermal product by measurement component.

the thermal wave penetrates into their domain. The difference between the linear approximation and an algorithmic fit to the equation (2) solution changes the thermal properties by less than 2%. The data in figure 5 show the solution to a gauge mounted on an idealized Pyrex backing material. These tests were repeated with copper and stainless steel as backing material to span a range of potential thermal properties. For each of these alternate setups, the linear solution varied from the complex processing by less than 2%. This advanced post processing with gauges mounted to different materials was necessary to validate assumption 1 in table 1. Since the fitting algorithm for the full solution is computationally intensive and was shown to minimally affect the results, the linear processing scheme was used for this work.

Worth noting, the out-of-phase third harmonic component (Y_3) as well as the first harmonic components (X_1, Y_1) can be linked to the thermal conductivity through similar, but independent processes [9]. For the current study, differences between the methods were 5.6%. The third in-phase harmonic (X_3, traditional 3-omega method) was chosen due to its established straightforward methodology as well as its insensitivity to phase errors and current stability errors [9].

5.3. *Thermal property error quantification*

There are three main error sources for the 3-omega method: fit uncertainty, precision error, and bias error. The fit uncertainty was estimated at 2% based upon the difference between the linear fit and the computational solution fit which correspond well to the work by Borca-Tasciuc *et al* [28]. The precision error was calculated based on a collection of 100 measurements for the same gauge and was found to be 0.42%. The bias uncertainty stems from various measurements that contribute to the final value. This was calculated using a perturbation method outlined by Moffat [29]. Figure 6 shows the relative impact of each of these bias-uncertainty contributors. These systematic errors arise from the uncertainty of measured parameters. For example, the error associated from the resistance value accounts for two-wire configuration of the HFGs in this study because the end application for this study (turbine blade heat transfer) is limited in available space. This error can be greatly reduced if a four-wire measurement technique is used instead.

Figure 6 shows that additional error sources are present in the thermal product quantification that are not present in the thermal conductivity. Specifically, the bias error of the measured voltage ($V_{3\omega}$) and the heater half width (b) increase the thermal product uncertainty. Therefore, the overall uncertainty of the thermal product is understandably higher than the thermal conductivity. From figure 6, the calculated bias errors for the thermal conductivity and thermal product were 2.0% and 4.4% respectively. When accounting for all error sources (precision, fit, and bias) through a root sum square, the overall uncertainty in the thermal conductivity and thermal product measurement is 2.9% and 4.9% respectively.

6. Thermal property results

This section presents the thermal property results from all available sensors using the 3-omega technique. First, the dielectric properties are quantified followed by the adhesive materials.

6.1. *Dielectric thermal property results*

Following the procedure outlined above in figure 5 using equation (4), the thermal conductivity and thermal diffusivity for seven individual gauges were characterized. This quantification was performed at each calibration setpoint shown in figure 4. A 10 mA current was supplied for the data presented below. Independent tests were repeated using excitation currents of 8.5 mA and 7 mA. Although not presented here, differences between the thermal property characterization from the excitation level was within the uncertainty for both the thermal product as well as the thermal conductivity.

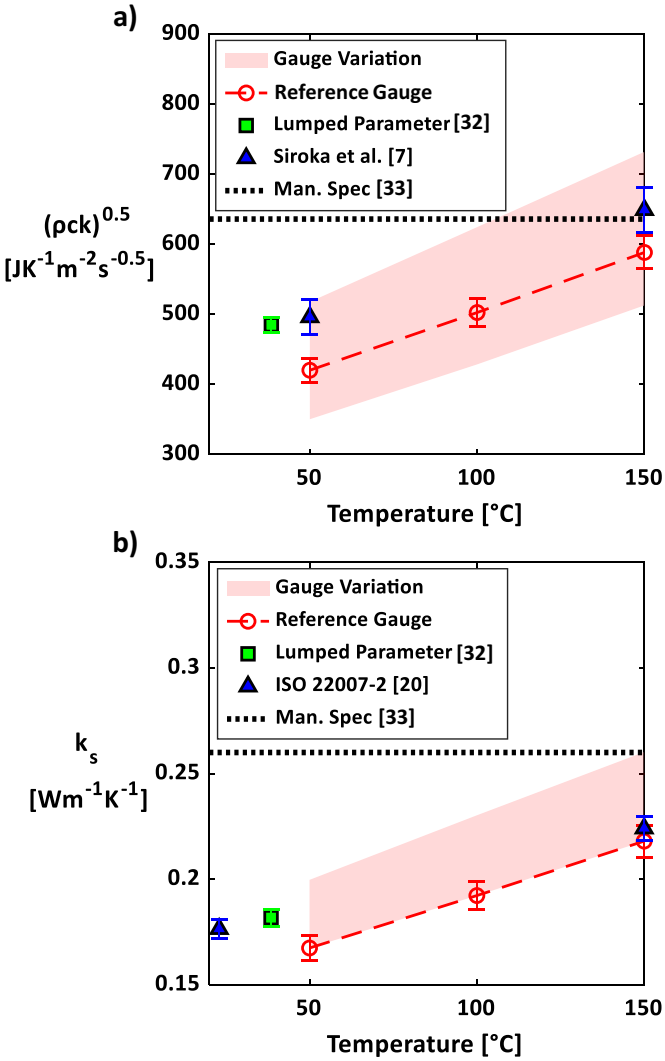

Figure 7. (a) Thermal conductivity results for seven different HFGs over a range of temperatures showing comparison to traditional methods. (b) Thermal product for seven HFGs over a range of temperatures comparing traditional methods to the current study.

Figure 7 illustrates the measurements for the example gauge used in the previous sections. The highlighted region shows the variation across all the tested gauges. The thermal conductivity quantified at 150 °C ranges from 0.22 to 0.26 ($Wm^{-1}K^{-1}$). Although a relatively narrow range, the thermal conductivity of the substrate is proportional to the mean heat flux value of the gauge. Therefore, any error in the thermal conductivity directly propagates to the measured heat flux. The variation in figure 7(a) serves to show that individual heat flux measurements could be affected by as much as 18% by improper gauge characterization from bulk value determination.

Although thermal conductivity is a parameter of interest on its own, the thermal product of the gauge affects the RMS error in the unsteady heat flux [1, 30, 31]. Similarly, the range illustrated in figure 7(b) shows that the RMS heat flux value could be affected by as much as 30% if only bulk values are used to reduce the heat flux. As a corollary, the 3-omega technique enables the thermal property determination of each individual gauge greatly reducing the errors from bulk value approximations.

Alongside the 3-omega quantification, figures 7(a) and (b) show previous bulk-value thermal property measurements [7, 20, 32, 33]. These processes were conducted by the authors for the same substrate material. Measurements compare well with the variation seen in the tested gauges indicating a benefit of the 3-omega method. The 3-omega method allows for thermal property information at each calibration setpoint while obtaining the electrothermal calibration. The other methods require significantly more effort for similar results that cannot be applied on an individual gauge basis. Figure 7 illustrates the importance to quantify these thermal properties over a range of temperatures enveloping all experimental operating conditions showing the variation with temperature for a given gauge over the tested conditions also varied by as much as 25% which is consistent with previous findings [7].

Both lumped parameter and 3-omega quantification schemes provide results that are often more accurate than the manufacturer specification. This is due to the fact that batch-to-batch variations exist and the substrate quantified by the manufacturer could be different than the material received. Therefore, these results suggest independent checks of material properties for individual gauges are necessary to substantially reduce the uncertainty of the measurement.

6.2. Adhesive thermal property results

Gauges of this type are commonly adhered to a test article. This adhesive layer acts as a thermal insulator yet is a critical parameter necessary to calculate heat flux from measured data. For this reason, it is essential to characterize the adhesive properties to relate measured heat flux to un-instrumented test articles. This is illustrated by Ni *et al* [23] who found that to match models to experiment, the adhesive layer as well as the substrate of the gauge must be considered.

Additional information about the backing adhesive can be acquired through the operation of the bottom-side thin-film RTD. The previous sections have illustrated that the thermal properties of the substrate can be quantified using the top thin film RTD. By means of this known information and exciting the bottom gauge in the same manner as described above for the 3-omega method, it is possible to calculate the thermal conductivity of the adhesive through a boundary mismatch approximation (BMA) [24, 34–37].

BMA assumes that the thermal transfer function of the system (in this case the adhesive and the substrate), can be summed in parallel. This summative approach yields equation (6) relating the measured apparent thermal conductivity of the system k_{sys} such that

$$k_{sys} = k_a + k_s \tag{6}$$

where k_a is the adhesive thermal conductivity and k_s is the substrate thermal conductivity, which was previously experimentally quantified. In equation (6), k_{sys} is measured through the backside 3-omega technique using equation (4). Because

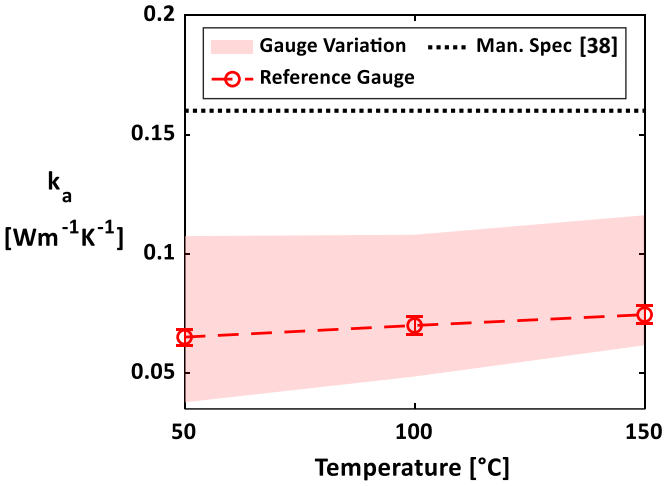

Figure 8. Schematic of experimental procedure and how it relates to time and temperature.

k_s is quantified through the top-side 3-omega method, it is possible to solve for the thermal conductivity of the adhesive, k_a. Note this technique can also be used to quantify the thermal diffusivity of the adhesive material [35, 37], but requires complex curve fitting algorithms. Since the high frequency heat flux components are damped by the gauge on the surface, and only the thermal conductivity affects the mean heat transfer rate, the quantification of thermal conductivity was prioritized instead of thermal diffusivity.

Figure 8 shows the results of these measurements. Similar to figure 7, the reference gauge and variation over the seven gauges is illustrated. Figure 8 also highlights the manufacturer specification [38]; notice that measured values in the current study are significantly lower than this specification. This discrepancy is attributed to the entrapment of air with the particular adhesive used in this study and its application method. Further, the difference in the specification and measured values illustrates the advantage of quantifying the adhesive layer *in-situ*.

7. Using the 3-omega technique for *in-situ* RTD calibration

As outlined in equations (1)–(4) and shown in the previous section, the 3-omega method links the thermal conductivity to the coefficient of resistance. When α_R is known during the calibration procedure, this relationship can be used to obtain the thermal properties of the gauge. However, the inverse of this relationship also offers utility for *in-situ* calibration checks of gauges. If the thermal properties are constant during operation (an assumption that will be evaluated experimentally in this study), it is therefore possible to back calculate α_R using the 3-omega method.

The following section will use data from the same reference gauge to test the feasibility of this theory for *in-situ* extraction of coefficient of resistance. To accurately apply this method, an initial assumption requires the thermal properties do not change with time. To test this assumption, the same thermal properties were measured before and after an annealing process of 72 h at 150 °C, as illustrated in figure 9. Since the coefficient of resistance is known to change with annealing, the α_R value was also calculated before and after the annealing process. These data were previously shown in figures 4(a) and (b), but will be referenced here again.

Shown in figure 10(a) is the thermal conductivity data collected for the same gauge before and after annealing with the measured coefficient of resistance (each data point is deduced from a 3-omega frequency sweep). On the right ordinate, the percent change in resistance is recorded for the same time interval. Notice that the resistance of the gauge changes more for the initial case than the annealed case. The results in figure 10(a) further illustrate the importance of annealing the gauge to obtain an accurate and repeatable calibration.

Figure 10(a) evaluates the assumption that the thermal properties remain unchanged over the 72 h annealing. The thermal conductivity measurements for the initial and annealed case illustrate that the mean data (in which the gauge was held slightly above 150 C for 72 h), shows differences of 0.1%. Therefore, when operating these gauges over extended periods, the thermal conductivity is also expected to remain unchanged which allows the coefficient of resistance to be back-calculated. Although expected, this validates the choice of polyimide as a dielectric for gauges of this type for its known property stability.

Unlike the experimental setup illustrated in figure 9, the coefficient of resistance will be unknown in practice. Therefore, it is beneficial to measure the thermal conductivity assuming the initial coefficient of resistance because it utilizes the exact measurement and post processing techniques. Figure 10(b) illustrates the calculated thermal conductivity based upon the assumption that the coefficient of resistance is constant. Under this assumption, there was a 4.3% difference in the thermal conductivity which correlates to an identical change in the coefficient of resistance.

Since the coefficient was measured in figure 10(a) and calculated in figure 10(b), it is possible to compare the measured to the calculated value. In this case, the difference between the calculated and measured coefficient of resistance would be identical to the change in thermal conductivity −0.1% (as illustrated by the mean value difference in figure 10(a)). This discrepancy is on the same order of magnitude as the uncertainty in the measured coefficient of resistance. Therefore, through this method, it is possible to accurately determine the coefficient of resistance.

There are several practical implications that arise from this technique. The most important is the ability to calibrate thin-film RTDs *in-situ*. As illustrated in figure 4(b), the electro-thermal calibration is linear, meaning that to define the calibration, one must know a single point and the slope of the line. The single point can be any single pair of resistance and temperature (R_{ref} and T_{ref}) for a platinum RTD under adiabatic conditions. For example, a nearby stable temperature device could be used to obtain T_{ref} while R_{ref} is the recorded gauge response before an experimental run. To obtain the calibration slope, the 3-omega method with the assumption of constant thermal properties from the calibration can then be used to

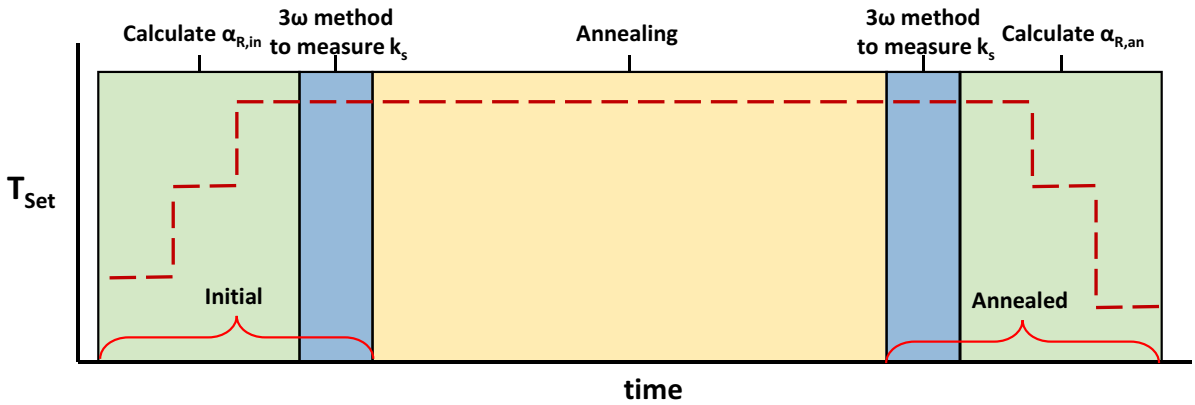

Figure 9. Measured thermal conductivity as a function of temperature for the calibration setpoints with highlighted gauge variation.

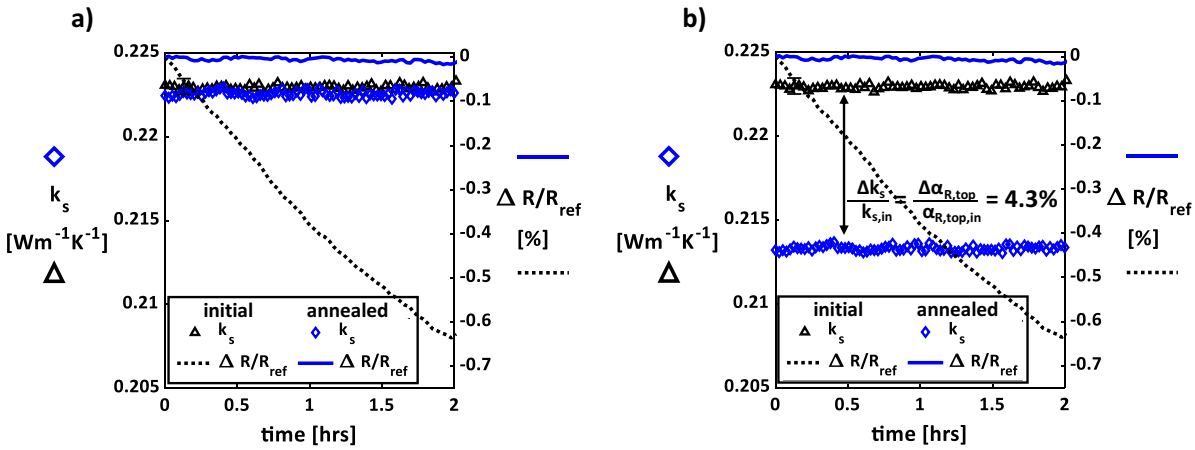

Figure 10. Thermal conductivity and resistance measurements for the sample gauge with (a) the assumption that $\alpha_{R,top}$ is constant and (b) the measured value of $\alpha_{R,top}$ using 3-omega.

calculate the coefficient of resistance. Therefore, an *in-situ* calibration can be performed as long as the T_{ref} value has a corresponding thermal conductivity from the oven calibration with the 3-omega technique. Theoretically, this method can also be extended to the bottom side gauge as long as both the adhesive properties and substrate properties are known following the exact same procedure, but substituting k_{sys} for k_a.

As a caution, it is imperative to validate the underlying assumption of constant thermal properties. This assumption is not only necessary for accurate heat flux measurements but is also critical to *in-situ* calibrations. Because the thermal conductivity is proportional to the coefficient of resistance, a percentage change in thermal conductivity will manifest as an equal error in the percentage change of the coefficient of resistance.

8. Conclusions

This work presents a novel calibration method for double-sided thin-film RTD HFGs. The proposed method allows for calibration of RTDs and thermal property determination in one integrated process, with additional benefits of characterizing thermal properties on a per-sensor basis. These thermal properties are necessary inputs when solving the unsteady conduction equation to deduce heat flux. These parameters are also the largest drivers of measurement uncertainty. Therefore, by designing a double-sided thin-film HFG capable of applying the 3-omega technique for thermal property determination, more accurate heat flux can be calculated.

To this end, this study outlines the design considerations for implementing the calibration procedure, highlighting that if proper care is taken, the thermal conductivity of the substrate and the thermal product can be determined within 3% and 5%, respectively. Quantifying these thermal properties on a per-gauge basis negates the assumption that bulk thermal property values represent the material directly under the RTD. Through the quantification of seven distinct double-sided thin-film RTD HFGs, this bulk material assumption was found to contribute as much as a 30% error in deduced mean and unsteady heat flux.

This study also addresses the need for an *in-situ* calibration method for double-sided thin-film RTD HFGs. For semi-permanent installations like turbine vanes and blades, this provides substantial value. More frequent calibrations lower the uncertainty in the RTD measurements. Since the RTD temperature values are used as the boundary conditions to solve the unsteady conduction equation and deduce heat flux, the

more frequent calibrations enabled by this proposed technique thereby also reduce the uncertainty in heat flux. To apply an *in-situ* calibration, it must be assumed that the substrate thermal properties are not degrading with time. This study showed that for a runtime of 72 h at 150 °C, the polyimide substrate displayed no measurable property changes, allowing an *in-situ* method to apply. When applying this technique, deduced α_R values differed from the measured α_R by 0.1%.

Overall, this study demonstrates the importance of proper substrate thermal property determination and recommends a calibration procedure to reduce uncertainty in measured heat flux quantities. The grouping of the 3-omega method and gauges of this type leads to improved gauge accuracy and novel *in-situ* calibration methods.

Data availability statement

The data that support the findings of this study are available upon reasonable request from the authors.

Acknowledgments

The authors would like to recognize and thank Pratt & Whitney and the U.S. Department of Energy National Energy Technology Laboratory under Award No. DE-FE0025011 for supporting research presented in this paper. This report was prepared as an account of work sponsored by an agency of the United States Government. Neither the United States Government nor any agency thereof, nor any of their employees, makes any warranty, express or implied, or assumes any legal liability or responsibility for the accuracy, completeness, or usefulness of any information, apparatus, product, or process disclosed, or represents that its use would not infringe privately owned rights. Reference herein to any specific commercial product, process, or service by trade name, trademark, manufacturer, or otherwise does not necessarily constitute or imply its endorsement, recommendation, or favoring by the United States Government or any agency thereof. The views and opinions of authors expressed herein do not necessarily state or reflect those of the United States Government or any agency thereof.

ORCID iD

Shawn Siroka https://orcid.org/0000-0001-9405-3004

References

[1] Epstein A H, Guenette G R, Norton R J G and Yuzhang C 1986 High-frequency response heat-flux gauge *Rev. Sci. Instrum.* **57** 639–49

[2] Guo S M, Spencer M C, Lock G D, Jones T V and Harvey N W 1995 The application of thin film gauges on flexible plastic substrates to the gas turbine situation *ASME Turbo Expo* 95-GT-357

[3] Epstein A H, Guenette G R and Norton R J G 1985 The design of the MIT blowdown turbine facility *GTL Report 183*

[4] Hodak M P 2010 Quantification of fourth generation kapton heat flux gauge calibration performance Ohio State University Thesis

[5] Piccini E, Guo S M and Jones T V 2000 The development of a new direct-heat-flux gauge for heat-transfer facilities *Meas. Sci. Technol.* **11** 342–9

[6] Anthony R J, Clark J P, Kennedy S W, Finnegan J M, Johnson D, Hendershot J and Downs J 2011 Flexible non-intrusive heat flux instrumentation on the AFRL research turbine *ASME Turbo Expo* GT2011–46853

[7] Siroka S, Berdanier R A, Thole K A, Chana K, Haldeman C W and Anthony R J 2020 Comparison of thin film heat flux gauge technologies emphasizing continuous-duration operation *J. Turbomach.* **142** 1–10

[8] Cahill D G 1990 Thermal conductivity measurement from 30 to 750 K: the 3ω method *Rev. Sci. Instrum.* **61** 802–8

[9] Dames C and Chen G 2005 1Ω, 2Ω, and 3Ω methods for measurements of thermal properties *Rev. Sci. Instrum.* **76** 1–14

[10] Anthony R J, Jones T V and LaGraff J E 2005 High frequency surface heat flux imaging of bypass transition *J. Turbomach.* **127** 241

[11] Celestina R, Sperling S, Christensen L, Mathison R, Aksoy H and Liu J, 2020 Development of new single and high-density heat-flux gauges for unsteady heat transfer measurements for a rotating transonic turbine *ASME Turbo Expo* GT2020–14527

[12] Sperling S, Celestina R, Christensen L, Mathison R, Aksoy H and Liu J, 2020 Variation of cooling mass flow rate and its effect on unsteady aerodynamic and heat transfer performance of a rotating turbine stage *AIAA Propulsion and Energy Forum*

[13] Ooten M K, Anthony R J, Lethander A T and Clark J P 2016 Unsteady aerodynamic interaction in a closely coupled turbine consistent with contrarotation *J. Turbomach.* **138** 1–13

[14] Chana K, Cardwell D and Jones T 2013 A review of the Oxford turbine research facility *ASME Turbo Expo* GT2013–95687

[15] Anthony R J, Finnegan J and Clark J P 2020 Phantom cooling effects on rotor blade surface heat flux in a transonic full scale 1+1/2 stage rotating turbine *ASME Turbo Expo* GT2020–15836

[16] Zhang J, Nagao Y, Kuwano S and Ito Y 1997 Microstructure and temperature coefficient of resistance of platinum films *Japan. J. Appl. Phys.* **36** 834–9

[17] Tiggelaar R M, Sanders R G P, Groenland A W and Gardeniers J G E 2009 Stability of thin platinum films implemented in high-temperature microdevices *Sens. Actuators* A **152** 39–47

[18] Chung G S and Kim C H 2008 RTD characteristics for micro-thermal sensors *Microelectron. J.* **39** 1560–3

[19] Zribi A, Barthès M, Bégot S, Lanzetta F, Rauch J Y and Moutarlier V 2016 Design, fabrication and characterization of thin film resistances for heat flux sensing application *Sens. Actuators* A **245** 26–39

[20] International Organization for Standardization (ISO) 2008 Plastics—determination of thermal conductivity and thermal diffusivity—part 2: transient plane heat source (Hot Disc) method *Int. Stand. ISO 22007–2*

[21] American Society for Testing and Materials (ASTM®) 2011 Standard test method for determining specific heat capacity by differential scanning *ASTM E1269*

[22] De Koninck D 2008 Thermal conductivity measurements using the 3-omega technique: application to power harvesting microsystems McGill University Thesis

[23] Ni R, Humber W, Fan G, Clark J P, Anthony R J and Johnson C J J, 2013 Comparison of predictions from conjugate heat transfer analysis of a film-cooled turbine vane to experimental data *ASME Turbo Expo* GT2013–94716
[24] Lubner S D, Choi J, Wehmeyer G, Waag B, Mishra V, Natesan H, Bischof J C and Dames C 2015 Reusable Bi-directional 3 ω sensor to measure thermal conductivity of 100-μm thick biological tissues *Rev. Sci. Instrum.* **86** 014905
[25] Dames C 2013 Measuring the thermal conductivity of thin films: 3 omega and related electrothermal methods *Annu. Rev. Heat Transf.* **16** 7–49
[26] Jacquot A, Lenoir B, Dauscher A, Stölzer M and Meusel J 2002 Numerical simulation of the 3ω method for measuring the thermal conductivity *J. Appl. Phys.* **91** 4733–8
[27] Gurrum S P, King W P and Joshi Y K 2008 A semianalytical solution for the 3ω method including the effect of heater thermal conduction *J. Appl. Phys.* **103** 113517
[28] Borca-Tasciuc T, Kumar A R and Chen G 2001 Data reduction in 3ω method for thin-film thermal conductivity determination *Rev. Sci. Instrum.* **72** 2139–47
[29] Moffat R J 1982 Contributions to the theory of single-sample uncertainty analysis *J. Fluids Eng.* **104** 250
[30] Oldfield M L G 2008 Impulse response processing of transient heat transfer gauge signals *J. Turbomach.* **130** 021023
[31] Billiard N, Iliopoulou V, Ferrara F and Dénos R, 2002 Data reduction and thermal product determination for single and multi-layered substrate thin-film gauges *Symp. on Measuring Techniques in Transonic and Supersonic Flow in Cascades and Turbomachines*
[32] Siroka S, Berdanier R A, Thole K A, Haldeman C W and Chana K S 2018 Penn State thin film heat flux gauge capabilities *ASME Turbo Expo Poster*
[33] DuPont 2018 Personal communication
[34] Grosse C, Abo Ras M, Varpula A, Grigoras K, May D, Wunderle B, Chapuis P O, Gomès S and Prunnila M 2018 Microfabricated sensor platform with through-glass vias for bidirectional 3-omega thermal characterization of solid and liquid samples *Sens. Actuators* A **278** 33–42
[35] Park B K, Park J and Kim D 2010 Note: three-omega method to measure thermal properties of subnanoliter liquid samples *Rev. Sci. Instrum.* **81** 3–6
[36] Chen F, Shulman J, Xue Y, Chu C W and Nolas G S 2004 Thermal conductivity measurement under hydrostatic pressure using the 3ω method *Rev. Sci. Instrum.* **75** 4578–84
[37] Moon I K, Jeong Y H and Kwun S I 1996 The 3ω technique for measuring dynamic specific heat and thermal conductivity of a liquid or solid *Rev. Sci. Instrum.* **67** 29–35
[38] 3M 2008 3M ™ ultrahigh temperature 100 HT adhesive transfer tape 9085 *Technical Data Sheet*